

# Simple Thermal Noise Estimation of OTA-based Switched-capacitor Filters

Christian Enz  
ICLAB, EPFL  
Neuchâtel, Switzerland  
christian.enz@epfl.ch

Francois Krummenacher  
EPFL  
Lausanne, Switzerland  
francois.krummenacher@epfl.ch

Assim Boukhayma  
CEA-LETI, Grenoble, France  
EPFL, Neuchâtel, Switzerland  
assim.boukhayma@epfl.ch

**Abstract**—This paper presents a new analytical method to simply estimate the integrated thermal noise in switched-capacitor filters (SCF). It is shown how the Bode theorem, which is theoretically valid only for continuous-time passive filters, can be extended to also estimate the noise in active SCF built with operational transconductance amplifiers (OTAs).

## I. INTRODUCTION

THE flicker noise due to the amplifiers used in switched-capacitor filters (SCF) can be significantly reduced thanks to the autozero technique [1]. The remaining noise is therefore ultimately dominated by the aliased noise due to sampling of the broadband thermal noise coming from the amplifiers and switches [1], [2]. Although today it is possible to simulate the noise of SCF [3], it remains difficult to have a 1<sup>st</sup>-order analytical expression to estimate the noise sufficiently accurately, in order to optimize the circuit [4]. This paper presents a new analytical method to simply estimate the integrated thermal noise in SCF. It is shown how the Bode theorem [5], which is theoretically valid only for continuous-time passive filters, can be extended to also estimate the thermal noise in active SCF built with operational transconductance amplifiers (OTAs).

## II. NOISE MECHANISMS IN SC FILTERS

Fig. 1 shows a typical integrator, part of a larger SCF and implemented by an OTA having a transconductance  $G_{mi}$  and an integrating capacitor  $C_i$ . The integrator virtual ground is connected to a switched-capacitor (SC)  $C_{1i}$  and a directly coupled capacitor  $C_{2i}$ . The noise in the SCF is generated from the noise sources in the OTAs and switches which is then sampled on the SCs and then transferred to the filter output [6]. The continuous-time noise seen at the filter output node during each phase (also called the direct noise) adds to this sampled and transferred noise [6]. The noise sampled on all the SCs connected to the virtual ground of the  $OTA_i$  is modelled in Fig. 1 by a noise charge  $Q_{ni}$  injected into the virtual ground at the end of each phase  $\Phi$ . The variance of this noise charge  $Q_{ni}^2$  is then the sum of the variances of the noise charge due to the different noise sources active in each phase  $\Phi$  (switches and OTAs) and sampled at the end of each phase  $\Phi$  on each SC connected to the virtual ground of  $OTA_i$ .

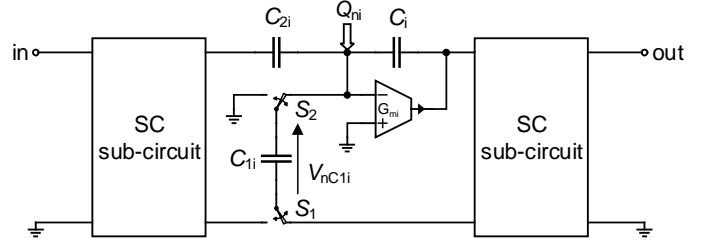


Fig. 1. General case of an SCF circuit that encompass at least one integrator.

$$Q_{ni}^2 = \sum_{\Phi} Q_{ni}^2|_{\Phi} \quad \text{with} \quad Q_{ni}^2|_{\Phi} = \sum_k C_{ki}^2 \cdot V_{nC_{ki}}^2|_{\Phi}. \quad (1)$$

The variances of the injected noise charges  $Q_{ni}^2|_{\Phi}$  are calculated in each phase from the variances of the voltages  $V_{nC_{ki}}$  across each switched-capacitor  $C_{ki}$  connected to the virtual ground  $i$ . The  $z$ -transfer function  $H_{ni}(z)$  from the injected noise charge  $Q_{ni}$  to the output is then evaluated. The variance of the output noise voltage is then given by [7]

$$V_{nout}^2 = \sum_i \frac{Q_{ni}^2}{C_i^2} \cdot \sum_{k=0}^{+\infty} h_{nik}^2 + V_{nout,direct}^2, \quad (2)$$

where  $h_{nik}$  is the  $k^{th}$  term of the impulse response corresponding to the transfer function from the virtual ground  $i$  to the output. In addition to the sampled noise, the variance of the continuous-time noise at the filter output  $V_{nout,direct}^2$  has to be added. The gain from the noise charge injector to the output can also be calculated directly from the transfer function  $H_{ni}(z)$  as [7]

$$\sum_{k=0}^{+\infty} h_{nik}^2 = \frac{1}{j2\pi} \oint_{\text{unit circle}} H_{ni}(z) \cdot H_{ni}(z^{-1}) \cdot z^{-1} dz. \quad (3)$$

Note that the later integral can be evaluated using the residues theorem according to [7]

$$\sum_{k=0}^{+\infty} h_{nik}^2 = \sum_k \text{Res} \{ H_{ni}(z) \cdot H_{ni}(z^{-1}) \cdot z^{-1} \}. \quad (4)$$

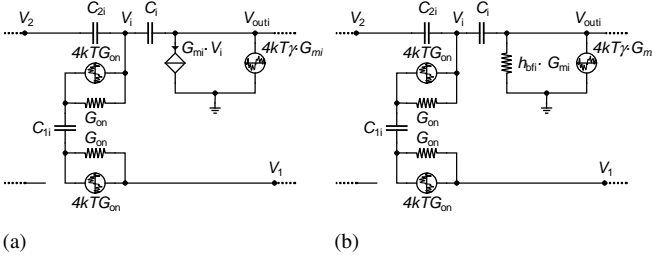


Fig. 2. a) Equivalent linear schematic of the integrator of Fig. 1 during charge transfer phase  $\Phi_2$ . b) Simplified equivalent linear schematic.

### III. SIMPLIFIED ESTIMATION OF THE THERMAL NOISE CHARGE VARIANCE

Calculating the thermal noise voltage variances  $V_{nC_{ki}}^2$  across each switched-capacitor  $C_{ki}$  connected to each virtual ground  $i$  can be complicated in most SCF circuits. In this Section, a new simple method is presented which extends the Bode theorem to the case of active SCF with OTAs.

Replacing all the MOS switches and OTAs in Fig. 1 by their linear equivalent circuit including their thermal noise sources leads to the schematic shown in Fig. 2a, where  $G_{on}$  is the on-conductance of the various switches which are assumed to be equal. The voltage  $V_i$  at the virtual ground node  $i$  is a linear combination of the output voltage of  $OTA_i$   $V_{outi}$  and the output voltages of the other OTAs coupled to node  $i$

$$V_i = h_{fbi}(\omega) \cdot V_{outi} + \beta_1(\omega) \cdot V_1 + \beta_2(\omega) \cdot V_2. \quad (5)$$

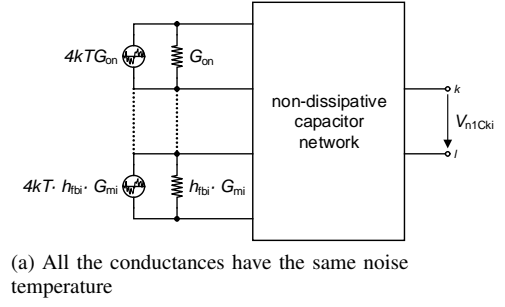
The transfer functions  $\beta_1(\omega)$  and  $\beta_2(\omega)$  are proportional to  $\alpha_1 = \frac{C_{1i}}{C_i}$  and  $\alpha_2 = \frac{C_{2i}}{C_i}$ , respectively. Assuming that the filter cut-off frequency is much lower than the sampling frequency implies that  $\alpha_1, \alpha_2 \ll 1$  and hence  $\beta_1(\omega), \beta_2(\omega) \ll 1$ . Consequently, the voltage  $V_i$  representing the  $OTA_i$  input is essentially a function of the OTA output voltage  $V_{outi}$

$$V_i \cong h_{fbi}(0) \cdot V_{outi}. \quad (6)$$

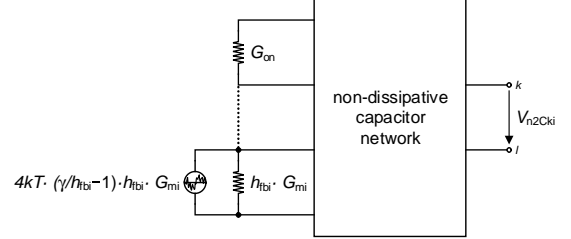
The voltage-controlled current source (VCCS) in Fig. 2a can then be replaced by a conductance of value  $h_{fbi} \cdot G_{mi}$  as depicted in Fig. 2b. Since the OTA thermal noise source has a power spectral density (PSD) proportional to  $G_{mi}$ , the equivalent circuit can actually be considered as passive. The noisy resistors of the switches have a noise temperature  $T$  whereas the noisy resistor of the equivalent conductance of the VCCS can be considered to have a temperature  $\frac{\gamma T}{h_{fbi}}$ , where  $\gamma$  is the noise excess factor of the  $OTA_i$ . Therefore, the noise voltage  $V_{nC_{ki}}^2$ , across capacitor  $C_{ki}$ , can be decomposed into the sum of two terms

$$V_{nC_{ki}}^2 = V_{n1C_{ki}}^2 + V_{n2C_{ki}}^2, \quad (7)$$

where  $V_{n1C_{ki}}^2$  corresponds to the noise observed when all the conductances have the same noise temperature as shown in Fig. 3a, whereas  $V_{n2C_{ki}}^2$  accounts for the excess noise present in the conductances  $\gamma_i \cdot h_{fbi} \cdot G_{mi}$  representing the OTAs as shown in Fig. 3b. Note that the schematic of Fig. 3b can



(a) All the conductances have the same noise temperature



(b) Excess noise temperature present in the conductances representing the OTAs

Fig. 3. Simplified schematic of an OTA based SCF.

be further simplified considering that  $G_{on} \gg h_{fbi} \cdot G_{mi}$  so that the on-conductances can be replaced by short-circuits without significant loss in accuracy. Therefore,  $V_{n1C_{ki}}^2$  can be calculated by applying the Bode theorem on the simplified schematics of Fig. 3a according to [5]

$$V_{n1C_{ki}}^2 = kT \cdot \left( \frac{1}{C_{\infty ki}} - \frac{1}{C_{0ki}} \right), \quad (8)$$

where  $C_{\infty ki}$  is the capacitance as seen between the nodes  $k$  and  $l$  when all switches and OTAs of the SC circuit are removed and  $C_{0ki}$  is the capacitance as seen between the nodes  $k$  and  $l$  when switches that are closed during the clock phase in consideration are replaced by short-circuits and all OTAs of the SC circuit have their output shorted to ground. In the same way,  $V_{n2C_{ki}}^2$  can be calculated as

$$V_{n2C_{ki}}^2 = kT \cdot \left( \frac{\gamma}{h_{fbi}} - 1 \right) \cdot \left( \frac{1}{C'_{\infty ki}} - \frac{1}{C_{0ki}} \right), \quad (9)$$

where  $C'_{\infty ki}$  is the capacitance as seen between the nodes  $k$  and  $l$  when switches that are closed during the clock phase in consideration are replaced by short-circuits and all OTAs of the SC circuit are removed. Note that the thermal noise variances  $V_{n1C_{ki}}^2$  and  $V_{n2C_{ki}}^2$  are simply obtained by inspection of the different equivalent circuits used to calculate  $C_{\infty ki}$ ,  $C'_{\infty ki}$  and  $C_{0ki}$  which are only made of connected capacitors. The total noise voltage variance (7) is then given by

$$V_{nC_{ki}}^2 = kT \cdot \left[ \frac{1}{C_{\infty ki}} - \frac{1}{C'_{\infty ki}} + \frac{\gamma}{h_{fbi}} \cdot \left( \frac{1}{C'_{\infty ki}} - \frac{1}{C_{0ki}} \right) \right] \quad (10)$$

where  $C_{\infty ki}$ ,  $C'_{\infty ki}$  and  $C_{0ki}$  are obtained by inspection of the three equivalent circuits depicted in Fig. 4.

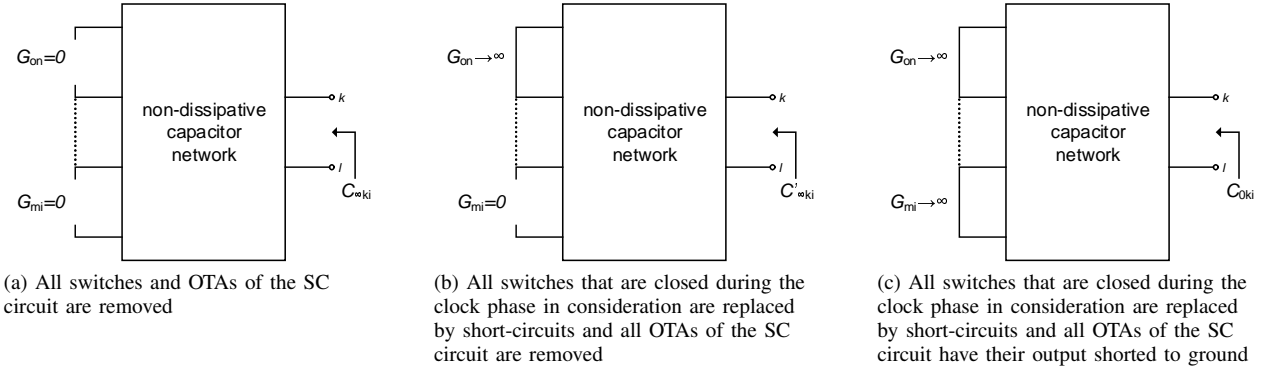


Fig. 4. Extension of the Bode theorem to OTA based SC filters.

#### IV. EXAMPLE: FIRST-ORDER LOW PASS SC FILTER

In order to better understand the noise calculation method presented above, this Section presents the example of a SC low pass filter as depicted in Fig. 5. The  $z$ -transfer function of this low-pass SCF is given by

$$H(z) = \frac{V_{in}(z)}{V_{out}(z)} = \frac{\alpha_1 \cdot z^{-1}}{1 + \alpha_2 - z^{-1}}, \quad (11)$$

where  $\alpha_1 = \frac{C_1}{C}$  and  $\alpha_2 = \frac{C_2}{C}$ . Note that  $\alpha_1$  and  $\alpha_2$  are much smaller than unity in the usual case where the cut-off frequency is much smaller than the sampling frequency. In order to simplify the calculations, it is considered that  $\alpha_1 = \alpha_2 = \alpha$ . At the end of phase  $\Phi_1$  and  $\Phi_2$ , the noise charges sampled on capacitors  $C_1$  and  $C_2$  are transferred to the integrating capacitor  $C$ . This sampled noise charge is modeled by the charge injector  $Q_n$  which injects a noise charge at the end of phase  $\Phi_2$  that represent the total noise charge injected onto the integrating capacitor  $C$  during one cycle (phase  $\Phi_1$  + phase  $\Phi_2$ ). The variance of this noise charge  $Q_n^2$  has to be calculated in each phase by evaluating the voltage variance on each switched-capacitor.

##### A. Noise variance estimation in phase $\Phi_1$

The method presented in the previous section is applied to calculate the noise voltage variances across the SCs connected to the virtual ground  $C_1$  and  $C_2$ . Thus  $V_{nC_1}^2|_{\Phi_1}$  and  $V_{nC_2}^2|_{\Phi_1}$  are calculated using (10). The calculation of capacitors  $C_\infty$ ,

$C'_\infty$  and  $C_0$  for the voltages across capacitors  $C_1$  and  $C_2$  at the end of phase  $\Phi_1$  is shown in Fig. 6 resulting in

$$V_{nC_1}^2|_{\Phi_1} = kT \cdot \left( \frac{1}{C_1} + 0 - 0 \right) = \frac{kT}{C_1}, \quad (12a)$$

$$V_{nC_2}^2|_{\Phi_1} = kT \cdot \left( \frac{1}{C_2} + 0 - 0 \right) = \frac{kT}{C_2}. \quad (12b)$$

The noise charge variance injected at the virtual ground at the end of phase  $\Phi_1$  can then be expressed as

$$Q_n^2|_{\Phi_1} = C_1^2 \cdot V_{nC_1}^2|_{\Phi_1} + C_2^2 \cdot V_{nC_2}^2|_{\Phi_1} = kT \cdot 2\alpha C. \quad (13)$$

##### B. Noise variance estimation in phase $\Phi_2$

Following the same steps as in the previous Section, the capacitors  $C_\infty$ ,  $C'_\infty$  and  $C_0$  for the voltages across capacitors  $C_1$  and  $C_2$  at the end of phase  $\Phi_2$  are first calculated using the schematics shown in Fig. 7. The feedback gain in phase  $\Phi_2$  is calculated using the equivalent circuit shown in Fig. 7a resulting in

$$h_{fb} = \frac{V}{V_{out}} = \frac{1 + \alpha}{1 + 2\alpha}. \quad (14)$$

By applying the method and assuming  $\alpha \ll 1$ , we find

$$V_{nC_1}^2|_{\Phi_2} = \frac{kT}{\alpha C} \cdot \frac{(1 + \alpha) \cdot (C_L + \alpha\gamma C)}{(\alpha)^2 C + C_L + \alpha \cdot (C + 2C_L)} \quad (15a)$$

$$V_{nC_2}^2|_{\Phi_2} = \frac{kT}{\alpha C} \cdot \frac{1 + \alpha + \gamma\alpha^2}{(1 + \alpha)^2} \simeq \frac{kT}{\alpha C}. \quad (15b)$$

Thus, the variance of the total noise charge injected in the virtual ground at the end of phase  $\Phi_2$  is given by

$$Q_n^2|_{\Phi_2} = kT \cdot \alpha C \cdot \left( 1 + \frac{\alpha\gamma C + C_L}{\alpha C + C_L(1 + 2\alpha)} \right). \quad (16)$$

##### C. Total noise variance estimation

The total noise charge variance injected at the end of every cycle into the virtual ground is then given by

$$Q_n^2 = Q_n^2|_{\Phi_1} + Q_n^2|_{\Phi_2}. \quad (17)$$

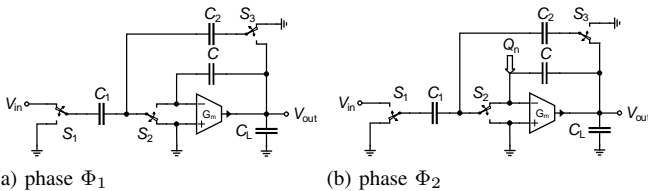


Fig. 5. SC low pass filter.

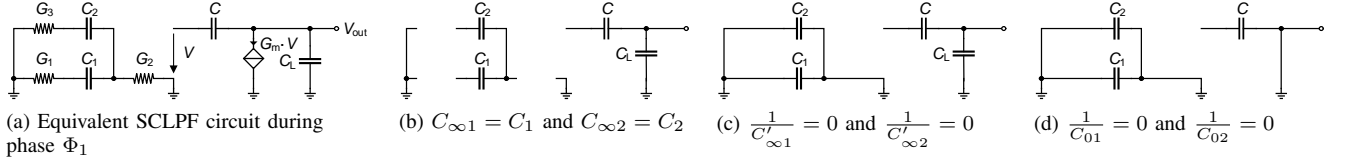


Fig. 6. Equivalent circuit schematics for noise variance calculation in Phase  $\Phi_1$ .

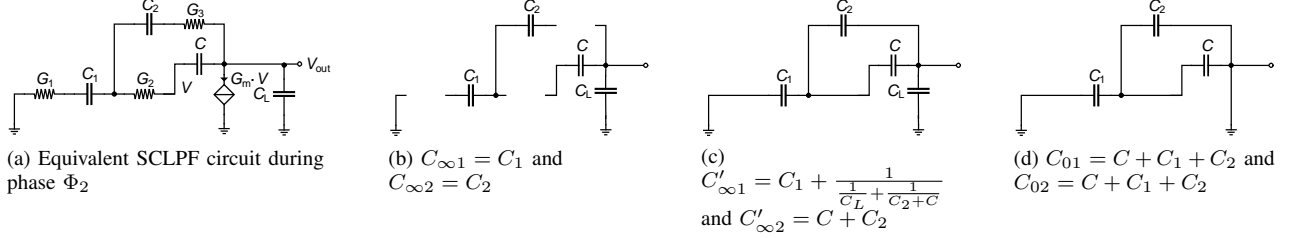


Fig. 7. Equivalent circuit schematics for noise variance calculation in Phase  $\Phi_2$ .

The noise charge  $Q_n$  is then transferred to the integrating capacitor  $C$ , generating an output voltage  $V_{out}$  calculated using (2) and given by

$$V_{out}(z) = H_n(z) \cdot \frac{Q_n}{C} \text{ with } H_n(z) = \frac{1}{1 + \alpha - z^{-1}}. \quad (18)$$

Thus,

$$\text{Res} \{ H_{ni}(z) \cdot H_{ni}(z^{-1}) \cdot z^{-1} \} = \frac{1}{\alpha(2 + \alpha)} \simeq \frac{1}{2\alpha}. \quad (19)$$

The output noise voltage variance is then calculated based on (3) and (4)

$$V_{nout}^2 \simeq \frac{3kT}{2C} + \frac{kT}{2C} \cdot \frac{\alpha\gamma C + C_L}{\alpha C + (1 + 2\alpha) \cdot C_L} + V_{nout,direct}^2. \quad (20)$$

For the 1<sup>st</sup>-order low pass filter of this example, the direct noise can be calculated as

$$V_{nout,direct}^2 = kT \cdot \frac{\gamma}{C_L + \alpha C}. \quad (21)$$

In order to validate this result, noise simulations are performed on the circuit of Fig. 5 for  $\alpha = 0.1$ ,  $C = 5pF$  and  $\frac{G_m}{G_{on}} = 0.1$  where  $G_m$  is the OTA transconductance and  $G_{on}$  the on-conductance of switches ( $G_{on} = G_1 = G_2 = G_3$  in the schematics of Fig. 6a and 7a). Both ELDO Transient noise and SpectreRF Pnoise simulations were performed. Fig. 8. shows the simulated RMS noise voltage at the output of the SCLPF, for  $C_L = C$ , together with the calculated noise using (20). It shows an excellent match between both the simulation and the analytical calculations, validating the presented noise estimation methodology.

## V. CONCLUSION

A simple method for the analytical estimation of thermal noise in OTA-based SCF is presented. The proposed method extends the Bode theorem to the case of OTA-based SCF. It

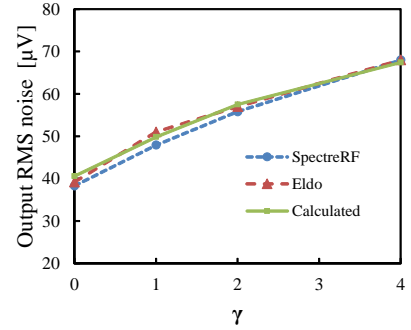


Fig. 8. Simulated output noise with SpectreRF Pnoise and Eldo Transient noise versus calculated noise in (24).

allows the sampled noise to be estimated by simple inspection of the SCF circuits. The new method is illustrated with the example of an OTA-based first-order SC low-pass filter. The estimated noise show an excellent matching compared to noise simulations using SpectreRF Pnoise and Eldo Transient-Noise.

## REFERENCES

- [1] C. C. Enz and G. C. Temes, "Circuit Techniques for Reducing the Effects of op-amp Imperfections: Autozeroing, Correlated Double Sampling, and Chopper Stabilization," *Proceedings of the IEEE*, vol. 84, no. 11, pp. 1584–1614, 1996.
- [2] F. Krummenacher, "Micropower Switched Capacitor Biquadratic Cell," *IEEE J. of Solid-State Circuits*, vol. 17, no. 3, pp. 507–512, June 1982.
- [3] B. Murmann, "Thermal Noise in Track-and-Hold Circuits: Analysis and Simulation Techniques," *IEEE Solid-State Circuits Magazine*, vol. 4, no. 2, pp. 46–54, Spring 2012.
- [4] R. Schreier, J. Silva, J. Steensgaard, and G. C. Temes, "Design-oriented Estimation of Thermal Noise in Switched-capacitor Circuits," *IEEE Trans. on Circuits and Systems I*, vol. 52, no. 11, pp. 2358–2368, Nov. 2005.
- [5] H. W. Bode, *Network Analysis and Feedback Amplifier Design*. New York: van Nostrand Company, 1945.
- [6] C. A. Gobet and A. Knob, "Noise Analysis of Switched Capacitor Networks," *IEEE Trans. on Circuits and Systems*, vol. 30, no. 1, pp. 37–43, Jan. 1983.
- [7] B. Furrer, "Rauschen von Filtern mit geschalteten Kapazitten," PhD, ETHZ, Date 1983, no. 7284.